Structural studies of bacterial enzymes and their relation to antibiotic resistance mechanisms

Lauren Maltz

Washington University in St. Louis, lmaltz@wustl.edu, Dated: August 5, 2015

Keywords: Crystal structure, Aminoglycoside, Oxacillinase, Carbapenem, Phosphotransferase, Antibiotic resistance

Abstract

By using protein crystallography and X-ray diffraction, structures of bacterial enzymes were solved to gain a better understanding of how enzymatic modification acts as an antibacterial resistance mechanism. Aminoglycoside phosphotransferases (APHs) are one of three aminoglycoside modifying enzymes that confer resistance to the aminoglycoside antibiotics via enzymatic modification, rendering many drugs obsolete. Specifically, the APH(2") family vary in their substrate specificities and also in their preference for the phosphate donor (ADP versus GDP). By solving the structures of members of the APH(2") family of enzymes, we can see how domain movements are important to their substrate specificity. Our structure of the ternary complex of APH(2")-IIIa with GDP and kanamycin, when compared to the known structures of APH(2")-IVa, reveals that there are real physical differences between these two enzymes, a structural finding that explains why the two enzymes differ in their preferences for certain aminoglycosides. Another important group of bacterial resistance enzymes are the Class D β-lactamases. Oxacillinase carbapenemases (OXAs) are part of this enzyme class and have begun to confer resistance to 'last resort' drugs, most notably carbapenems. Our structure of OXA-143 shows that the conformational flexibility of a conserved hydrophobic residue in the active site (Val130) serves to control the entry of a transient water molecule responsible for a key step in the enzyme's mechanism. Our results provide insight into the structural mechanisms of these two different enzymes.

1. Introduction

With the widespread use of antibiotics, bacteria are rapidly becoming resistant to antibiotics. It only takes two years of antibiotic exposure for some bacteria to evolve resistance to the antibiotics. Thus, antibiotics are no longer able to fight off certain bacterial infections. Increasing antibacterial resistance means more people are dying of previously treatable infections because the drugs are losing effectiveness or are rendered obsolete. As the prevalence of antibiotic resistance continues to climb, it poses a serious hazard to public health. The primary goals of research on both antibacterial and enzymatic resistance are to find its various mechanisms, to create new drugs that are not inactivated by these resistance mechanisms, and to discover a way to decrease or reverse resistance in order to allow current antibiotics to successfully treat serious bacterial infections.

The most common mechanisms of antibacterial resistance are diminished cell entry, active efflux, target alteration, and the enzymatic inactivation or modification of the drugs (Pascale et al., 2010). We are focusing on the bacterial enzymes responsible for the deactivation of two families of antibiotics, the aminoglycosides and the β-lactams. In the first case, aminoglycoside modifying enzymes (AMEs) are those that cause high levels of resistance to aminoglycoside

This material is based upon work supported by the U.S. Department of Energy, Office of Science, Office of Workforce Development for Teachers and Scientists (WDTS) under the Science Undergraduate Laboratory Internship (SULI) program, under Contract No. DE-AC02-76SF00515.

antibiotics by three different methods. Aminoglycosides are especially important to investigate because of the promiscuity of their target profiles and the variety of life threatening diseases that they can be used to treat from genetic disorders to endocarditis (Ramirez et al., 2010). Examples of these aminoglycoside antibiotics include gentamicin and kanamycin, which are currently rendered obsolete due to the consequences of resistance. When β-lactams and aminoglycoside antibiotics are combined for treatment, they produce a synergistic effect (Ramirez et al., 2010).

The three families of aminoglycoside modifying enzymes whose nomenclatures describe their methods of enzymatic modification are: acetylytransferases (AACs), nucleotidyltransferases (ANTs), and phosphotransferases (APHs). Aminoglycoside phosphotransferases are named for their ability to confer resistance to aminoglycoside antibiotics by transferring phosphate groups to free hydroxyl groups on the drugs. Looking at APH(2")-IIIa, for example, the 2" represents the site of the hydroxyl group on the antibiotic that is phosphorylated, and in general this number represents the location of antibiotic modification. The Roman numeral signifies the enzyme's substrate specificity, as no two enzymes have the same specificity profile. The lowercase letter that follows tells the enzyme's amino acid composition, distinguishing different genetic sequences with the same substrate specificity.

In the second case, bacteria produce over 1300 diverse enzymes called β-lactamases which exist as four classes: A, B, C and D. Class D β-lactamase enzymes, also known as oxacillinases or OXA enzymes, are capable of deactivating a wide range of β-lactam antibiotics, including "last resort" drugs such as the carbapenems. OXA carbapenemases are mostly found in gram-negative bacteria and are potentially contributing to the resistance of carbapenems in clinical isolates. Their host species include *Acinetobacter baumannii* and *A. pittii*, which are becoming important human pathogens due primarily to the occurrence of β-lactam resistance. Carbapenem resistance has increased due to the spread of such OXA-type β-lactamases (Leonard et al., 2012 and Evans et al., 2014).

All APH(2") enzymes were previously considered to solely use ATP as the phosphate donor source for antibiotic modification. However, in recent studies it has been found that ATP is in fact a poor substrate for two of these enzymes, APH(2")-Ia and APH(2'')-IIIa, in which GTP is exclusively used as the *in vivo* phosphate source (Toth et al., 2009). ATP is a poor source for APH(2")-IIIa because a tyrosine residue in the active site, Tyr-92, acts as a so-called 'gatekeeper' and blocks the specific binding of ATP (Smith et al., 2012). Similarly, Tyr100 acts as a gatekeeper residue in APH (2")-Ia. Two other enzymes in the APH(2") family, APH(2")-IIa and APH(2")-IVa, both have an almost equal ability to use GTP and ATP, and these enzyme have 'gatekeeper' residues that are smaller than tyrosine and are able to move to allow ATP binding (APH(2")-IIa uses Met85 and APH(2")-IVa uses Phe95). We are delving further into APH(2") family's GTP binding capabilities, enzymatic structure, and resistance mechanism in which enzymes modify and inactivate the antibiotics. Looking at structural and molecular mechanisms of these enzymes will offer clues as to why the adenosine triphosphate (ATP) is preferred, show parts of the enzyme that are involved in resistance, and how the bacteria become resistant. It will also allow for the comparison of the structural components of different enzymes.

By using the Stanford Synchrotron Radiation Lightsource (SSRL) beamlines at the SLAC National Accelerator Laboratory and protein crystallography methods, we grow protein crystals, collect data using the beamlines, and solve the structures of two important bacterial resistance enzymes, the apo-form of OXA-143 and the ternary GTP-kanamycin complex of APH(2")-IIIa.

2. Materials and Methods

Data sets for OXA143 and APH(2")-IIIa were processed using HKL2000, imosflm, and XDS/XSCALE. Data collection and statistics are presented in Table 1 for APH(2")-IIIa and in Table 2 for OXA-143. XDS/XSCALE consistently gave the best results for both data sets and structures.

Table 1: APH(2")-IIIa Data Collection Statistics

Maximum resolution (d_{min}) (Å)	1.35
Relections to d_{min} (observed/unique)	1026717/71703
R_{merge} [a] (%)	5.2 (88.5) [b]
I/σ_I	30.3 (3.2)
Completeness (%)	100.0 (100.0)
CC½ [c]	100.0 (83.4)
Multiplicity	14.5 (13.6)
Wilson B ($Å^2$)	13.6
Space group	$P2_12_12$
Unit cell dimensions (Å)	a=77.17, b=58.98, c=70.85
R-factor / R_{free} (%) [d]	15.38 / 18.12
R_{all} (%) [e]	15.52
Total atoms - protein / solvent	2455 / 308
B factors	
- protein chain ($Å^2$)	20.3
- solvent ($Å^2$)	29.2
rms deviation from ideality	
- bond distances (Å)	0.006
- bond angles (°)	1.20
Ramachandran plot [f]	
- residues in most favored regions (%)	97.52
- residues in additionally allowed regions (%)	2.48

[a] $R_{merge} = \Sigma|I - \langle I \rangle| / \Sigma I \times 100$, where I = the observed intensity and $\langle I \rangle$ is the mean intensity. [b] Numbers in parentheses relate to the highest resolution shell, 1.32 -1.30 Å. [c] Percentage of correlation between intensities from random half-sets of data (Karplus & Diederichs, 2013). [d] $R = \Sigma||F_o| - k|F_c|| / \Sigma|F_o| \times 100$. R_{free} was calculated with 5% of the reflections. [e] Final R-factor calculated with all data using no sigma cutoff. [f] Calculated with the program PROCHECK (Chen *et al.*, 2010)

Table 2: OXA-143 Data Collection Statistics

Maximum resolution (d_{min}) (Å)	1.15
Reflections to d_{min} (observed/unique)	499245/149425
R_{merge}[a] (%)	5.8 (62.3)[b]
I/σ_I	11.45 (1.9)
Completeness (%)	96.1 (87.8)
CC½[c]	99.9 (73.4)
Multiplicity	3.4 (3.0)
Wilson B ($Å^2$)	9.0
Space group	$P2_1$
Unit cell dimensions (Å)	a=40.95, b=62.33, c=87.10, β=91.7°
R-factor / R_{free} (%)[d]	13.75 / 16.22
R_{all} (%)[e]	13.87
Total atoms - protein / solvent	1980 (A), 1954 (B) / 567
B factors	
- protein chain ($Å^2$)	12.2 (A), 18.1(B)
- solvent ($Å^2$)	30.3
rms deviation from ideality	
- bond distances (Å)	0.005
- bond angles (°)	1.042
Ramachandran plot[f]	
- residues in most favored regions (%)	97.80
- residues in additionally allowed regions (%)	1.54

[a] $R_{merge} = \Sigma|I - \langle I \rangle| / \Sigma I \times 100$, where I = the observed intensity and $\langle I \rangle$ is the mean intensity. [b] Numbers in parentheses relate to the highest resolution shell, 1.18 – 1.15 Å. [c] Percentage of correlation between intensities from random half-sets of data (Karplus & Diederichs, 2013). [d] $R = \Sigma||F_o| - k|F_c|| / \Sigma|F_o| \times 100$. R_{free} was calculated with 5% of the reflections. [e] Final R-factor calculated with all data using no sigma cutoff. [f] Calculated using the program PROCHECK (Chen *et al.*, 2010).

2.1 APH(2")-IIIa

The APH(2")-IIIa ternary complex structure was solved at a resolution of 1.35 Å by molecular replacement using the program MOLREP from the CCP4 program suite, using the wild-type APH(2")-IIIa as the starting model. The structure was then refined using REFMAC and PHENIX, and the program COOT was for interactive model building into electron density maps (see Table 1 for final statistics).

2.2 OXA-143

The OXA-143 sequence was compared with the sequences of OXA-23, -24, -48, -51, and -58. Table 3 shows the sequence identity percentages among these enzymes, with the highest similarity existing between OXA-143 and OXA-24 (PDB code 3ZNT). The CCP4 program CHAINSAW was used to convert OXA-24 into a pseudo OXA-143 model by pruning non-conserved residues between the two enzymes so that the sequences are consistent. This pseudo OXA-143 was then used to solve the structure using MOLREP, and the resultant structure was refined initially with REFMAC from the CCP4 programs. Refinement was later switched to PHENIX (see Table 2 for final statistics).

Table 3: Pairwise Sequence Identities of OXA-23, 24, 48, 51, and 58 with OXA-143

Structure	Pairwise Sequence Identity (%)	PDB code[a]
OXA-23	60.7%	4JF6
OXA-24	87.6%	3G4P
OXA-48	30.7%	3HBR
OXA-51	64.0%	4ZDX
OXA-58	51.4%	4OH0

[a] From http://www.rcsb.org

3. Results and Discussion

3.1 APH(2")-IIIa

The ternary complex of APH(2")-IIIa with GDP and kanamycin shows how the substrate binds. APH(2")-IIIa is composed of two domains, an N-terminal domain and a C-terminal domain. The C-terminal domain can be further divided into two sub-domains, the core and the helical sub-domains. The GTP binding site is located between the N-terminal domain and the core subdomain. The aminoglycoside binding site is located between the core and helical subdomains (Figure 1)

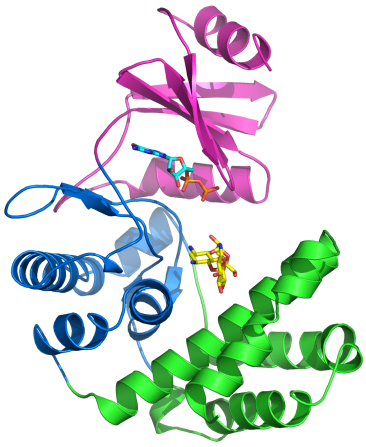

Figure 1. Ribbon representation of APH(2")-IIIa shows three structural domains, N-terminal (purple), central core (blue), and helical (green). The location of the GDP (cyan sticks) and the kanamycin (yellow sticks) are also shown.

Comparison of the APH(2")-IIIa structures with and without kanamycin shows that there is no movement of the helical domain relative to the core domain upon substrate binding. The same is known for APH(2")-IVa based on previous studies. However when APH(2")-IIIa is compared to APH(2")-IVa (PDB code 3SG9), there is a significant movement of the helical domain between the two enzymes (Figure 2). This domain movement is not due to the presence or lack of kanamycin but rather real conformational differences in the two structures. In addition, the kanamycin in APH(2")-IVa is closer to helical domain and slightly further away from the aspartate (ASP196) relative to APH(2")-IIIa. The structural differences observed support the known differences in the two enzymes substrate profiles and specificities.

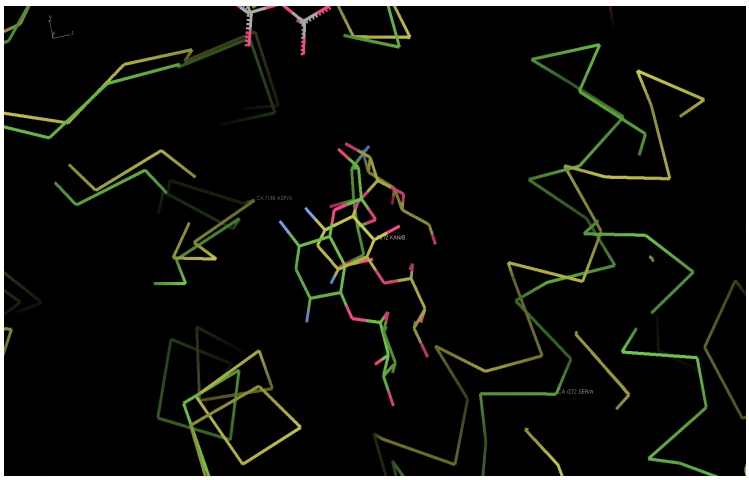

Figure 2. Stick representation of APH(2")-IIIa (yellow) and APH(2")-IVa (green) superimposed on each other, showing helical domain movement. The helical sub-domain shown on left and the core sub-domain shown on right of the substrate kanamycin.

3.2 OXA143

The OXA-143 structure has 240 amino acid residues, from 36 to 275. The molecule is composed of two structural domains with the non-contiguous N-terminal domain (residues 36-75 and 207-275) comprising a five-stranded β-sheet flanked by two α helices. The second domain is an all-α domain folded from a single contiguous piece of polypeptide (76-206). The active site is

in the cleft between the two structural domains and includes important catalytic residues Ser81, Lys84, Val130, Trp167, Ser219 and Arg261.

The mechanism of OXA-143 (and all known class A and D β-lactamases) is a two-step process as follows:

(1) Acylation: Acyl-enzyme intermediate $E + S' \rightleftharpoons E\text{-}S$,

(2) Deacylation : Breakdown of acyl-enzyme intermediate $E\text{-}S + H_2O \rightleftharpoons E + S^*$

where S'=active substrate, S*=deactived substrate.

Step (2) requires a water molecule. It is typically both the rate-limiting step in the reaction and the step over which the enzyme has the most control. Each of the residues listed above has a different role in carrying out the acylation/deacylation process. Ser81 forms the initial covalent bond in Step (1) to produce the acyl-enzyme intermediate. Together, Ser128 and Lys218 form a hydrogen bond connecting the two domains and maintaining the shape and structure of the active site. Ser219 and Arg261 bind to the substrate and lock it into place so that the process can occur. Trp167 stabilizes the position of the Lys84 side chain which, in turn, orients a water molecule in the correct position for the deacylation step. Most notably, and uniquely to OXA-143, the role of Val130 appears to be control of the occupancy of this deacylating water molecule. The side chain of Val130 exists in two conformations, and its location near Lys84 and the deacylating water molecule means the water molecule can only be present with one of these Val130 conformations (Figure 3). One conformation of the valine creates open space to allow the water to be present thereby allowing the deacylation step, whereas the other side chain conformation blocks the water site and would switch off deacylation. Hence the Val130 side chain is controlling access of this water and the reaction rate of the enzyme deacylation step. This presence of this transient water shows that OXA-143 has a different control mechanism than has previously been seen with other OXA enzymes.

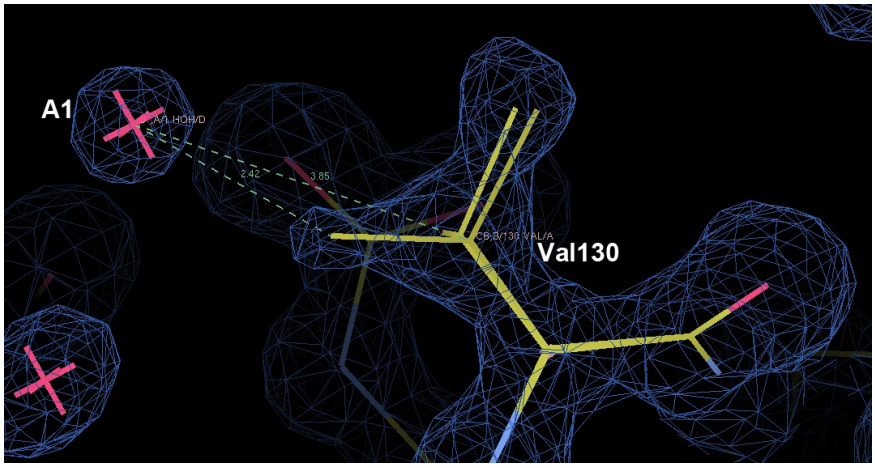

Figure 3. Stick representation of deacylating water, A1, and the two conformations of amino acid residue Val130. In one conformation of Val130 (conf. B), a carbon atoms is 2.42 Å away from A1, whereas in the second conformation (conf. A) the closest carbon atoms is 3.85 Å away. A1 cannot come closer than 3.2 Å to a carbon atom, therefore it can only be present in conjunction with Val130 conf. A.

4. Conclusion

Each member of the APH(2”) family is named differently because of their distinct substrate profiles, supported by the real structural differences that we have observed between members of the APH(2”) enzyme family. It was found that OXA-143 has a similar structure to other OXA enzymes. However, it differs from other OXA enzymes with respect to its control mechanisms. In OXA-143, Val130 controls access to the deacylating water and the rate of Step (2) of the enzyme mechanism. In the future, potential new drugs against the OXA enzymes must account for the many different control mechanisms among the OXAs, posing a greater obstacle in creating unique inhibitors. With the potential of making future drugs and alternative options for treatment, we hope to stop antibacterial resistance from continuing along its increasingly destructive path.

5. Acknowledgements

This work is based upon research conducted at the Stanford Synchrotron Radiation Lightsource at SLAC National Accelerator Laboratory, a national user facility, operated by the United States Department of Energy and Stanford University. Thank you to Clyde Smith for your guidance and support, and welcoming me into the lab for the summer. Thank you to University of Notre Dame and Sergei Vakulenko for the purified proteins.

6. References

Chen, V.B., Arendall, W.B., Headd, J.J., Keedy, D.A., Immormino, R.M., Kapral, G.J., Murray, L.W., Richardson, J.S., Richardson, D.C. (2010). MolProbity: All-atom structure validation for macromolecular crystallography. Acta Crystallogr. D66, 12-21.

De Pascale, G., Wright, G.D. (2010). Antibiotic resistance by enzyme inactivation: from mechanisms to solutions. ChemBioChem, 11, 1325-1334.

Evans, B.A., Amyes, S.G.B. (2014). OXA β-Lactamases. Clinical Microbiology Reviews, 27, 241-263.

Karplus, P.A., Diederichs, K. (2012). Linking crystallographic model and data quality. Science 336, 1030-1033.

Leonard, D.A., Bonomo, R.A., Powers, R.A. (2013). Class D β-lactamases: a reappraisal after five decades. Accounts of Chemical Research, 46, 2407-2415.

Smith, C.A., Toth, M., Frase, H., Vakulenko, S.B., Byrnes, L.J. (2012). Aminoglycoside 2” phosphotransferase IIIa (APH(2”)-IIIa) prefers GTP over ATP. J. Biol. Chem. 287, 12893-12903.

Toth, M., Chow, J.W., Mobashery, S., Vakulenko, S.B. (2009). Source of phosphate in the enzymic reaction as a point of distinction among aminoglycoside 2”-phosphotransferases. J. Biol. Chem. 284, 6690-6696.

Ramirez, M.S., Tolmasky, M.E. (2010). Aminoglycoside modifying enzymes. Elsevier Ltd. 13, 151-171.